Science Advances

AAAS

advances.sciencemag.org/cgi/content/full/2/9/e1501425/DC1

Supplementary Materials for

Room temperature stable CO_x-free H_2 production from methanol with magnesium oxide nanophotocatalysts

Zhengqing Liu, Zongyou Yin, Casandra Cox, Michel Bosman, Xiaofeng Qian, Na Li, Hongyang Zhao, Yaping Du, Ju Li, Daniel G. Nocera

Published 2 September 2016, *Sci. Adv.* **2**, e1501425 (2016)
DOI: 10.1126/sciadv.1501425

This PDF file includes:

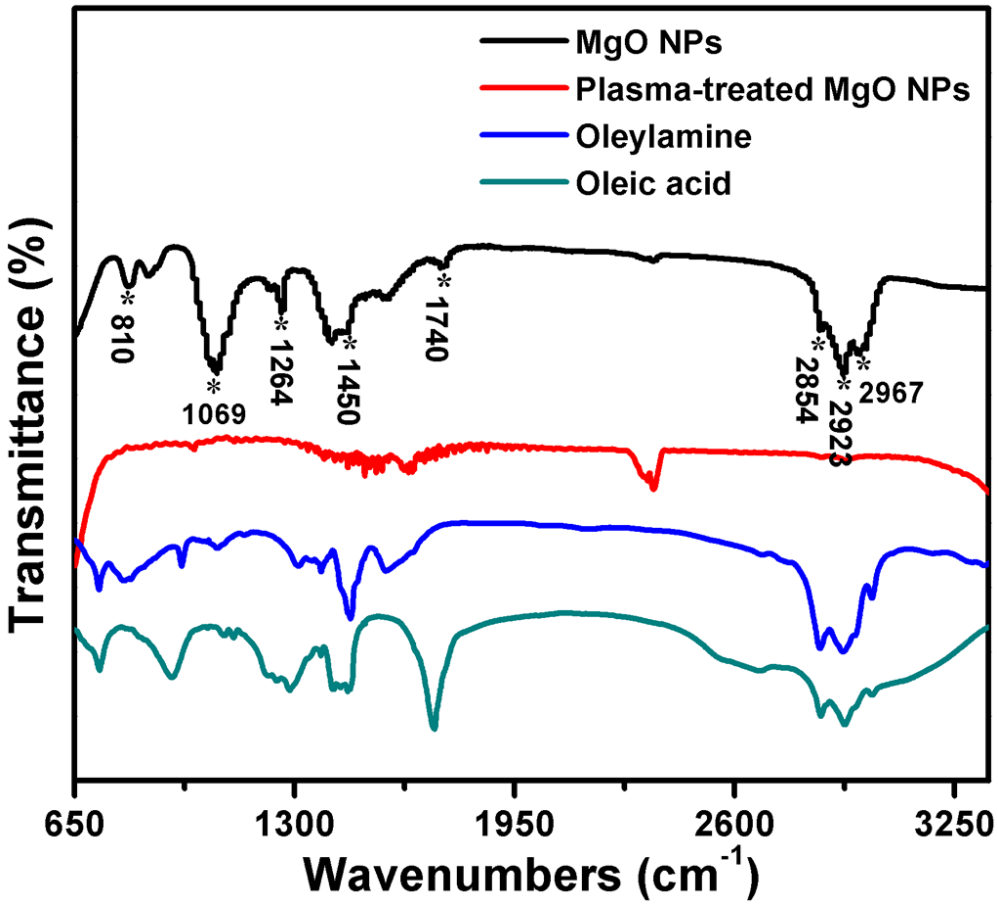

fig. S1. FTIR analysis of synthesized and oxygen plasma–treated MgO NPs. FTIR spectra (Nicolet 6700) of oleylamine, oleic acid, as-prepared MgO NPs and plasma-treated MgO NPs. The presence of acyclic C-H stretching at 2967 cm^{-1}, 2923 cm^{-1} and 2854 cm^{-1} indicate the co-existence of oleic acid and oleylamine. The peaks at 1740 cm^{-1} and 1450 cm^{-1} are assigned to C=O stretch and carboxylate (COO^{-}) stretch, implying the COO^{-} ligand exists on the nanocrystals surface. Additionally, the three sharp peaks at 1264, 1069 and 810 cm^{-1} in the IR spectrum of MgO NPs were indexed to C–N stretch of oleylamine, respectively. Based on the FTIR analysis of MgO NPs, it is confirmed that these MgO nanocrystals are coated by two kinds of organic molecule, oleylamine and oleic acid. Note here, after oxygen plasma treatment, the intensity of characteristic peaks of oleic acid and oleylamine obviously decreased, indicating a successful removal of organic capping ligands from the surface of MgO NPs.

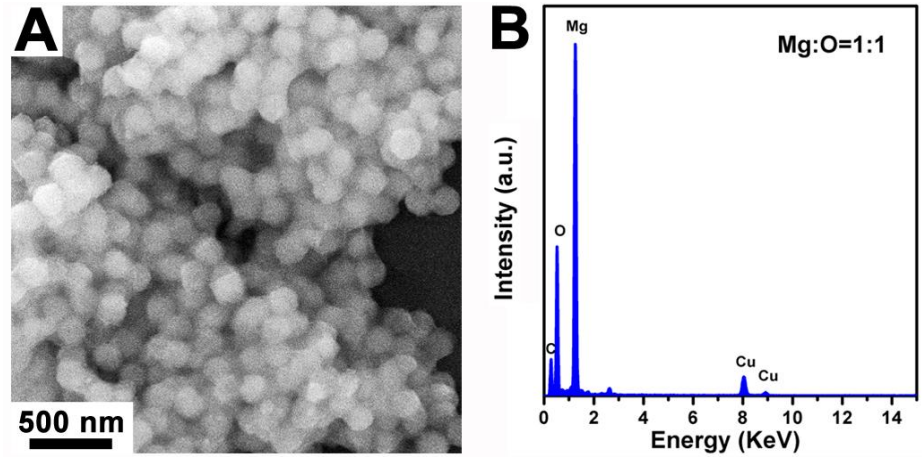

fig. S2. SEM image and EDX analysis of synthesized MgO NPs. (**A**) Scanning electron microscope (SEM) image and (**B**) energy-dispersive X-ray analysis (EDX) spectrum of MgO NPs with size of ~170 nm.

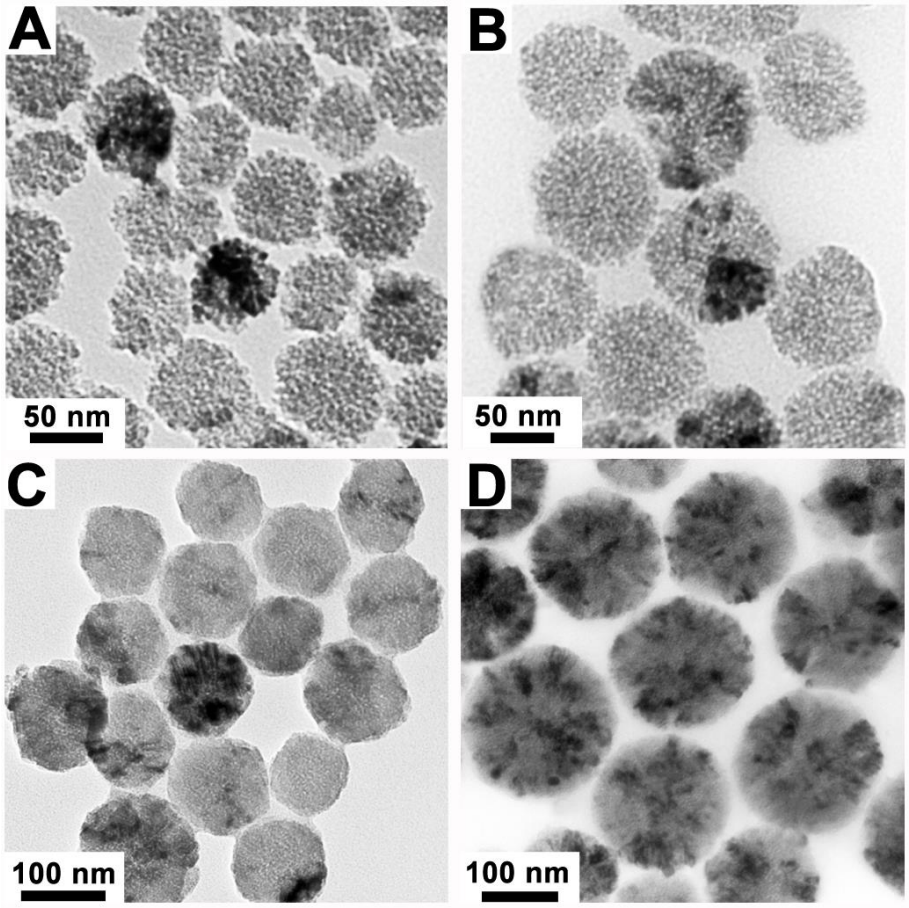

fig. S3. Temperature-dependent experiments of synthesized MgO NPs. TEM images of MgO NPs obtained from the thermolysis of 2 mmol $Mg(acac)_2 \cdot 2H_2O$ in OM/OA/ODE (4:1:5) at different temperature for same reaction time of 60 min. (**A**) 265°C, (**B**) 280°C, (**C**) 300°C, and (**D**) 320°C. From the TEM images, the average sizes of MgO NPs can be estimated to be (**A**) ~60 nm, (**B**) ~100 nm, (**C**) ~115 nm, and (**D**) ~170 nm, respectively.

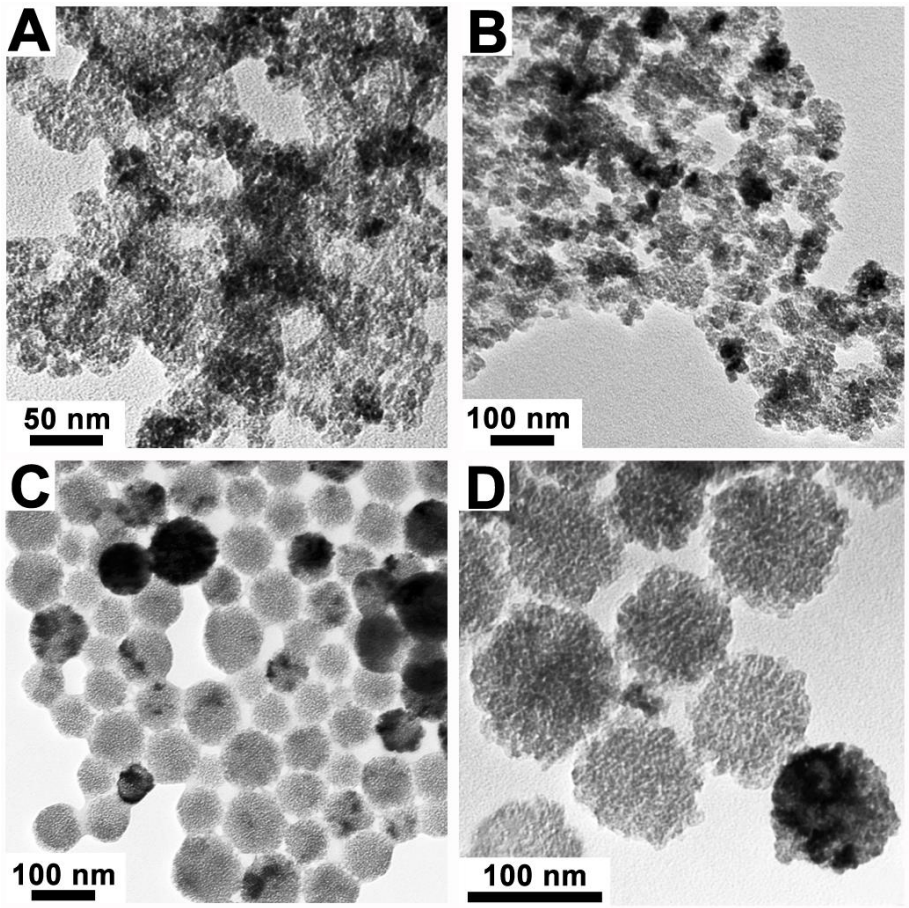

fig. S4. Solvent composition–dependent experiments of synthesized MgO NPs. TEM images of MgO NPs obtained from the thermolysis of 2 mmol of $Mg(acac)_2 \cdot 2H_2O$ in different mixed solvents at 280 °C for 30 min: (**A**) OM:ODE=1:1, (**B**) OM:OA:ODE=14:1:15, (**C**) OM:OA:ODE=8:1:9, and (**D**) OM:OA:ODE=2:1:3.

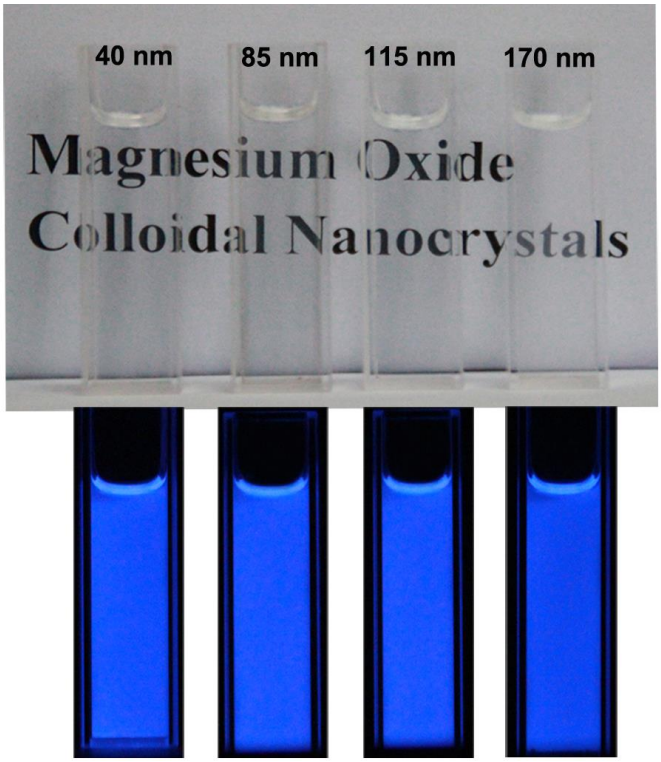

fig. S5. Digital photographs of different-sized MgO colloidal solution.
Photographs of 1 mg mL^{-1} porous MgO NPs dispersed in cyclohexane under ambient illumination (top) and under an irradiation of 365 nm UV light (bottom).

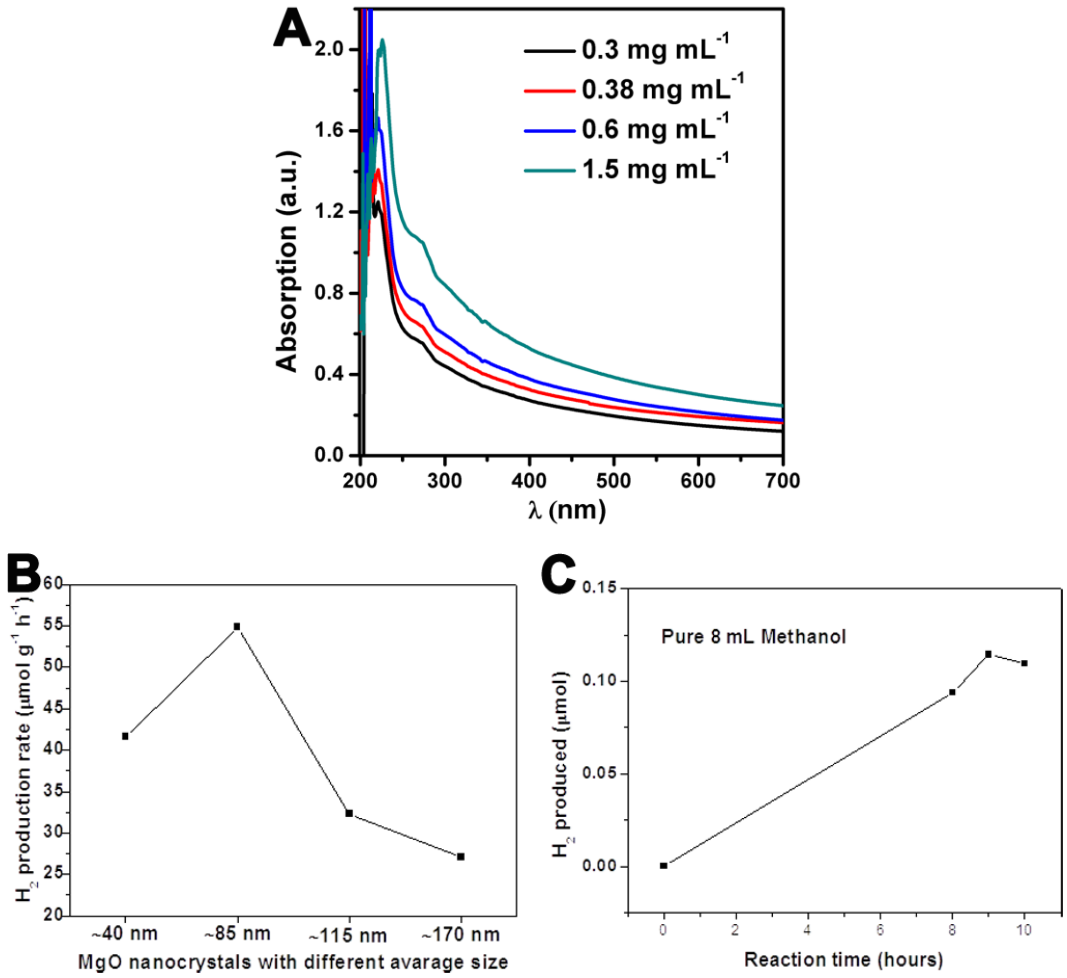

fig. S6. Optical properties for ~85 nm MgO nanocrystals and H_2 production from methanol photodecomposition. (A) Room temperature UV–vis absorption spectra of plasma-treated 85 nm sized MgO NPs in methanol with different concentrations. (B) H_2 production rate from MgO nanocrystals with different sizes (MgO concentration in methanol: 0.38 mg mL^{-1}). (**C**) H_2 produced from pure methanol without MgO under the same illumination conditions as used for the measurements in Fig. 4C.

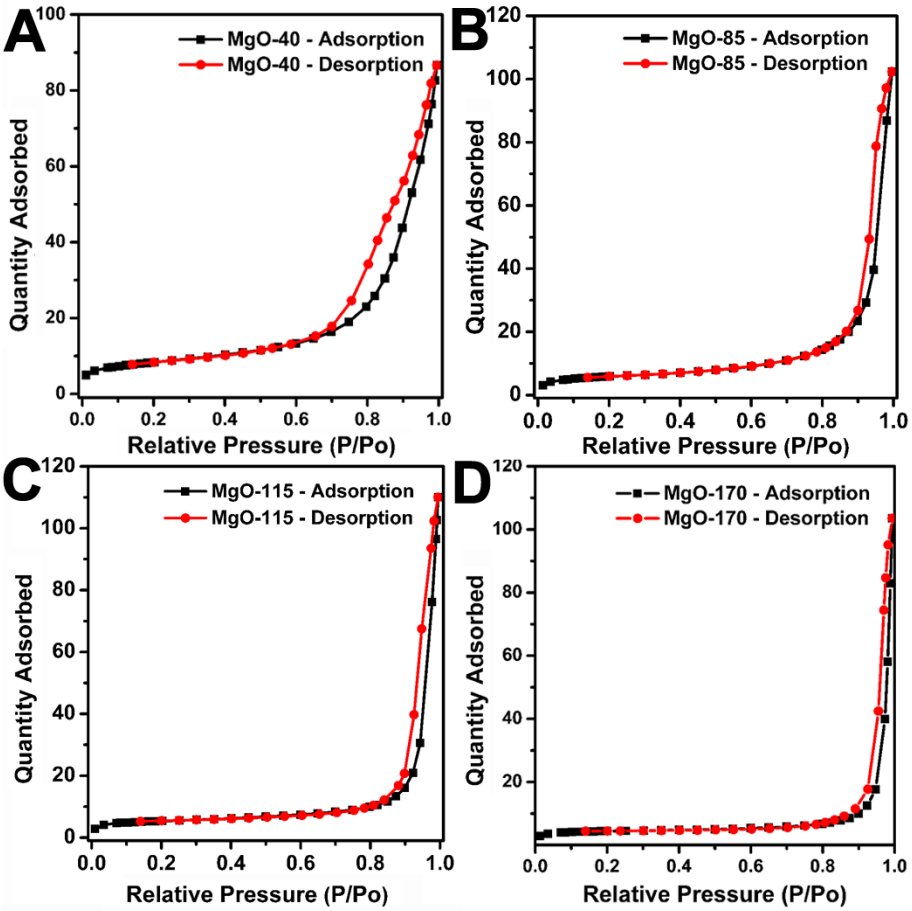

fig. S7. Specific surface area of four different-sized MgO NPs. Nitrogen adsorption and desorption isotherms measured at 77 K for MgO NPs with four different sizes, *i.e.* (**A**) ~40 nm, (**B**) ~85 nm, (**C**) ~115 nm and (**D**) ~170 nm, based on which the specific surface area is calculated by using the Brunauer-Emmett-Teller (BET) method.

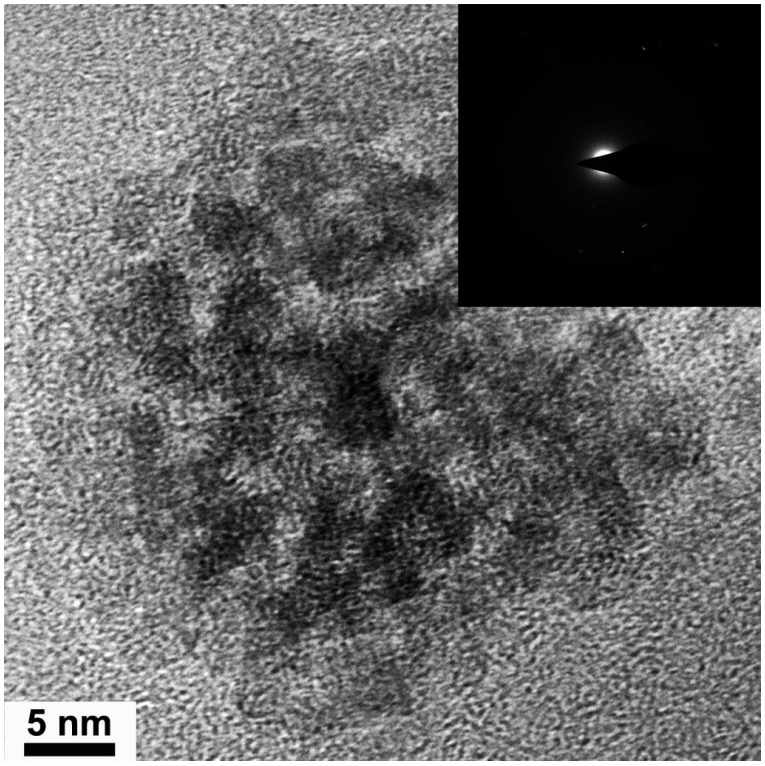

fig. S8. TEM and SAED images of an MgO NP with a size of 40 nm. TEM image of a single porous MgO nanoparticle with size of 40 nm, and the inset is the corresponding SAED image. As seen from SAED image, the ~40 nm sized MgO has low crystallinity degree.

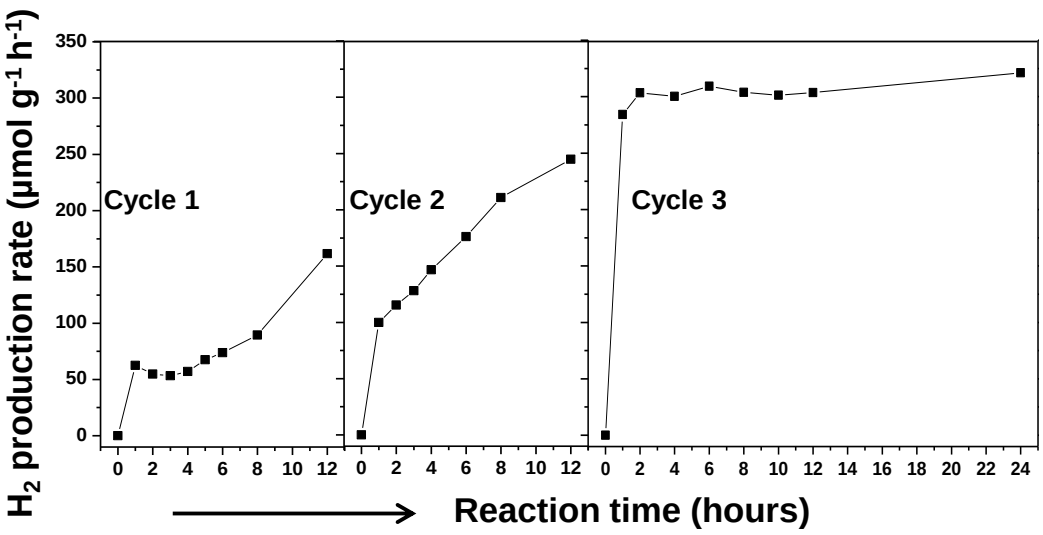

fig. S9. The rate pattern of H_2 production for ~85-nm MgO nanocrystals. H_2 production rate pattern for ~85-nm MgO nanocrystals based on the H_2 production results as presented in Fig. 4C.

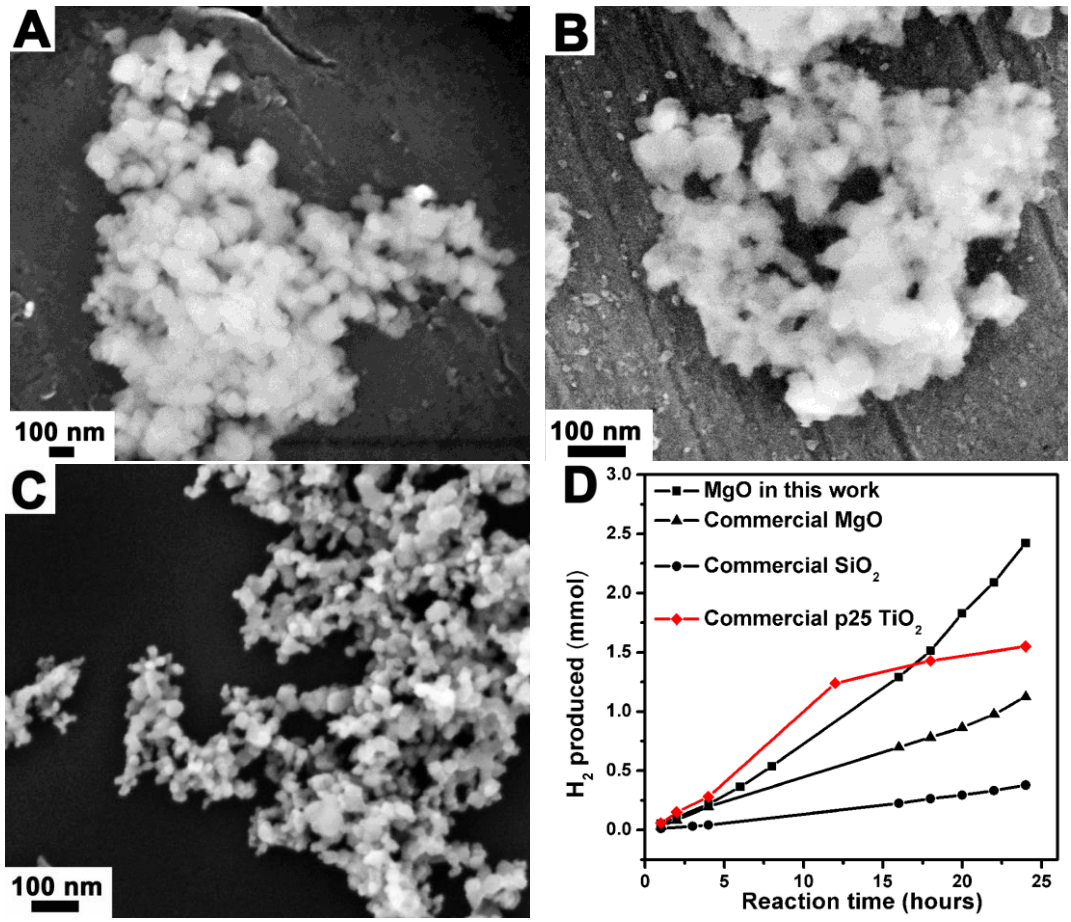

fig. S10. SEM analysis and H_2 production of commercial MgO, SiO_2, and TiO_2 (P25). The SEM images of commercial (A) MgO, (B) SiO_2, and (C) TiO_2 nanoparticles. (D) Comparison of H_2 production between MgO in this work, commercial MgO, commercial SiO_2 and commercial TiO_2 under the light illumination intensity of ca. 176 mW cm^{-2}.

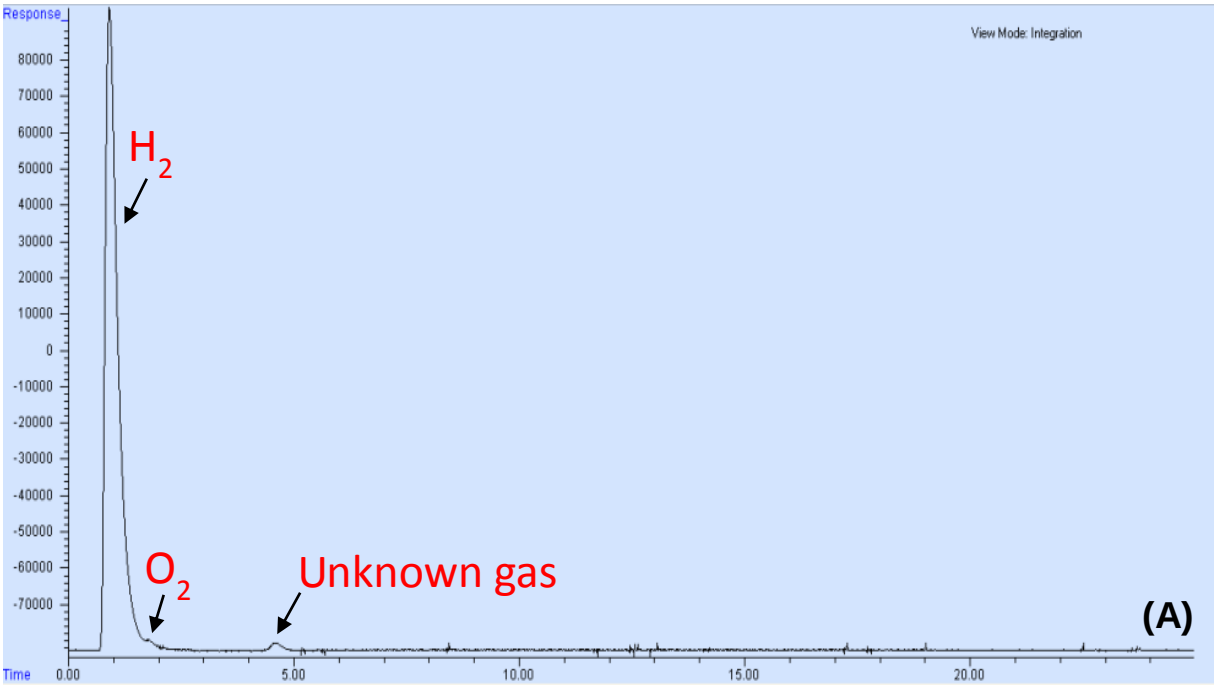
Response_
View Mode: Integration
80000
70000
60000
50000
40000
30000
20000
10000
0
-10000
-20000
-30000
-40000
-50000
-60000
-70000
H2
O2
Unknown gas
(A)
Time
0.00
5.00
10.00
15.00
20.00

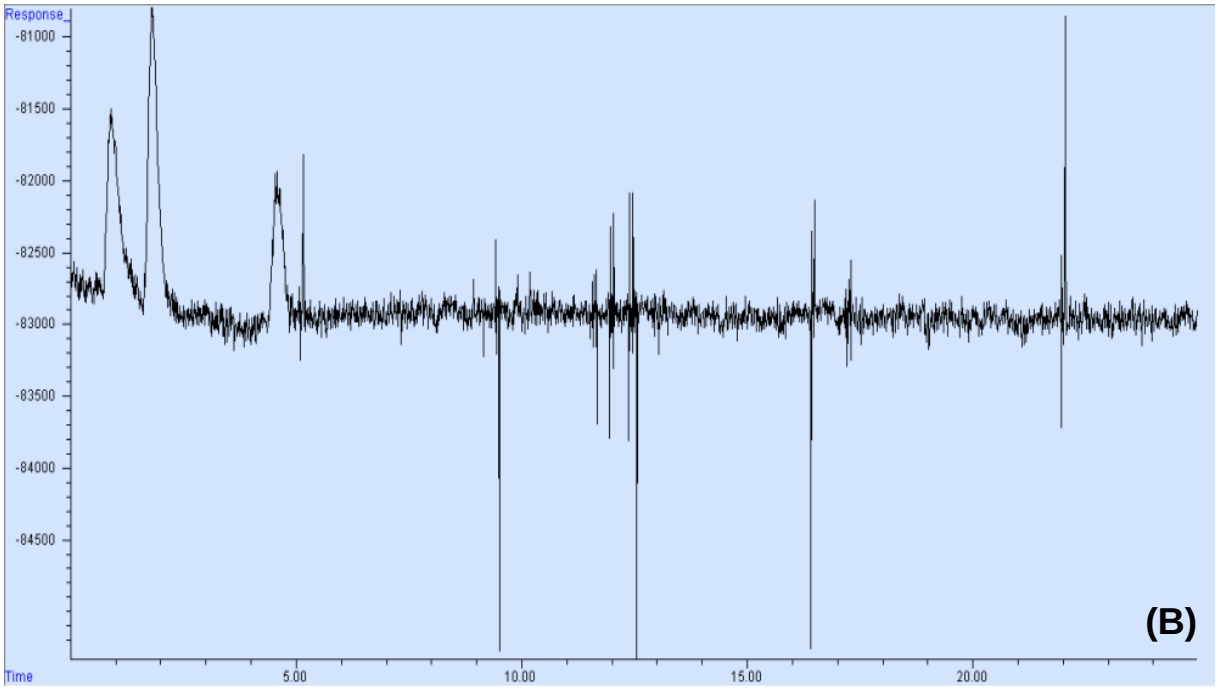
Response_
-81000
-81500
-82000
-82500
-83000
-83500
-84000
-84500
(B)
Time
5.00
10.00
15.00
20.00

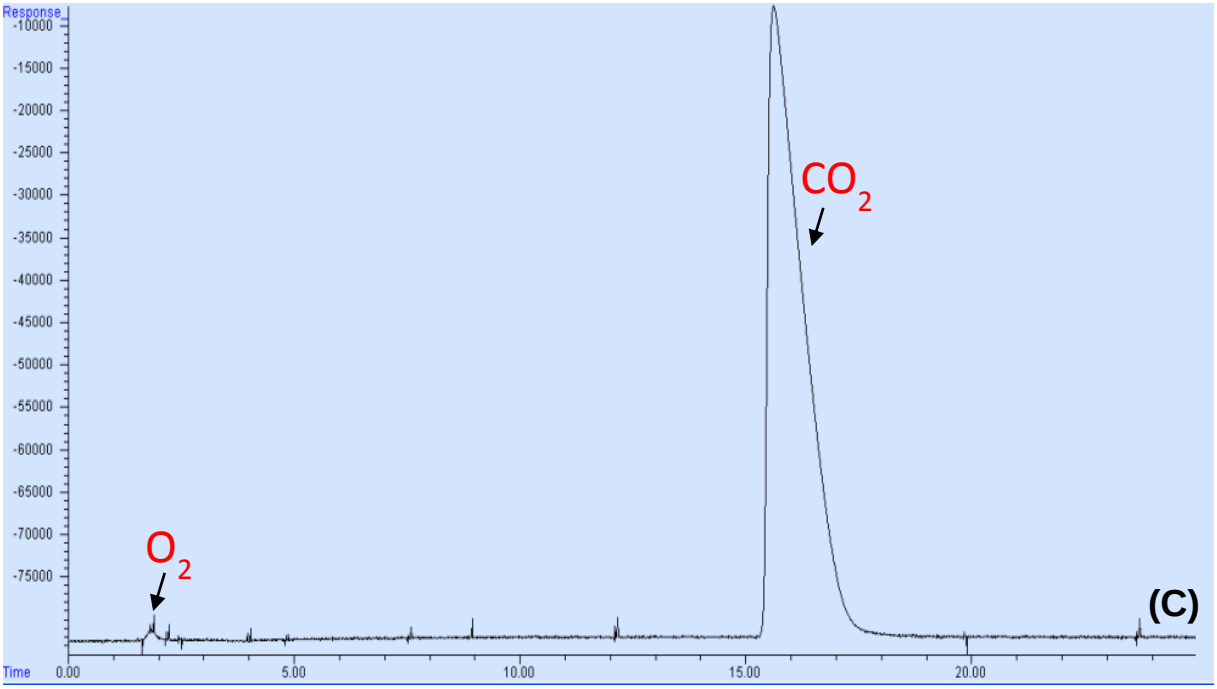

fig. S11. Chromatogram analysis of a mixture of gases. (**A**) 3mg MgO in 8 mL methanol after 48-hour photocatalytic reaction with 25-minute retention time in X-axis of chromatogram, (**B**) pure 8 mL methanol after 10-hour reaction, and (**C**) standard carbon dioxide (CO_2) gas.

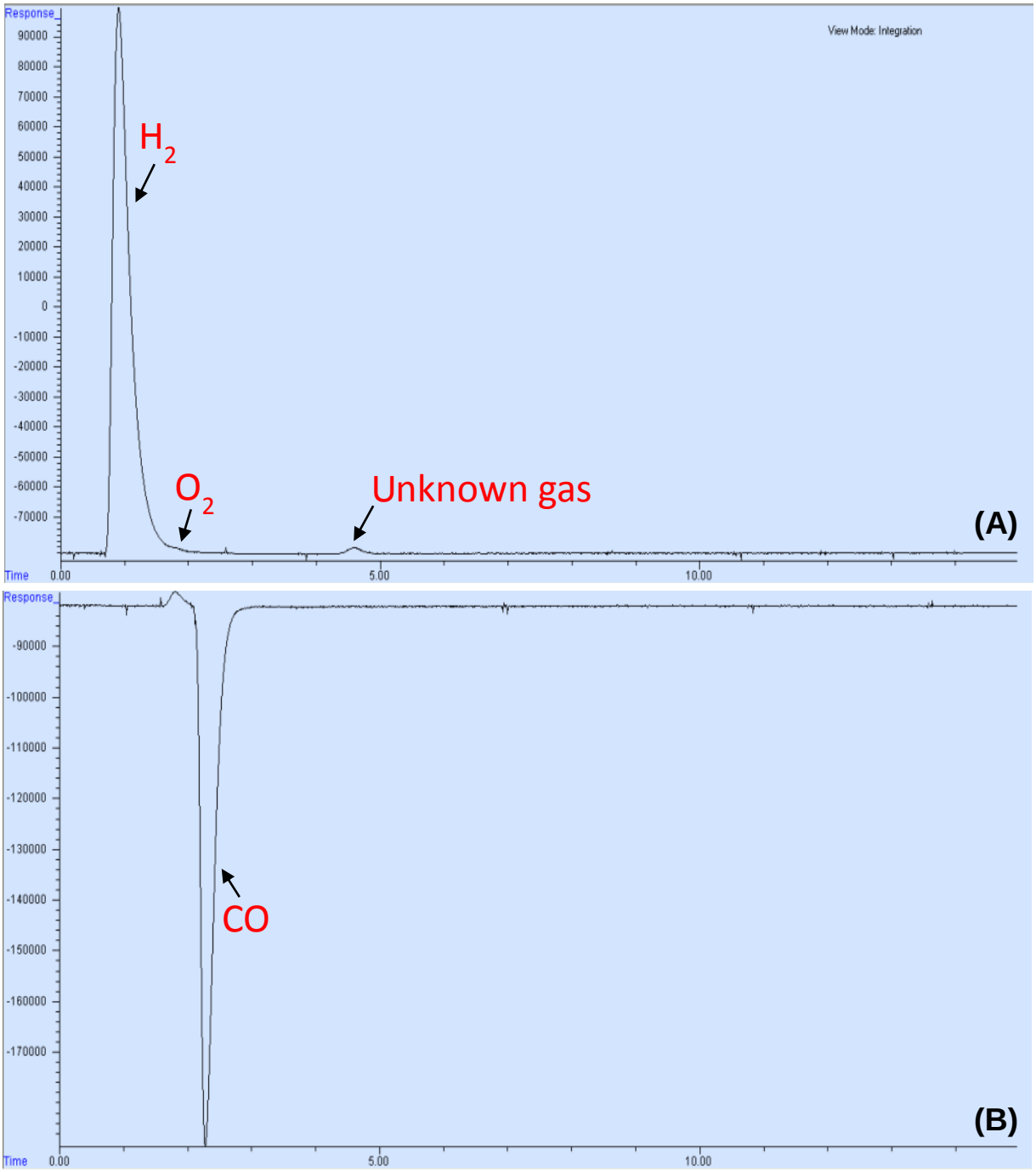

fig. S12. Chromatogram analysis of a mixture of gases. (**A**) 3mg MgO in 8 mL methanol after 48-hour photocatalytic reaction with 15-minute retention time in X-axis of chromatogram, and (**B**) the standard carbon monoxide (CO) gas.

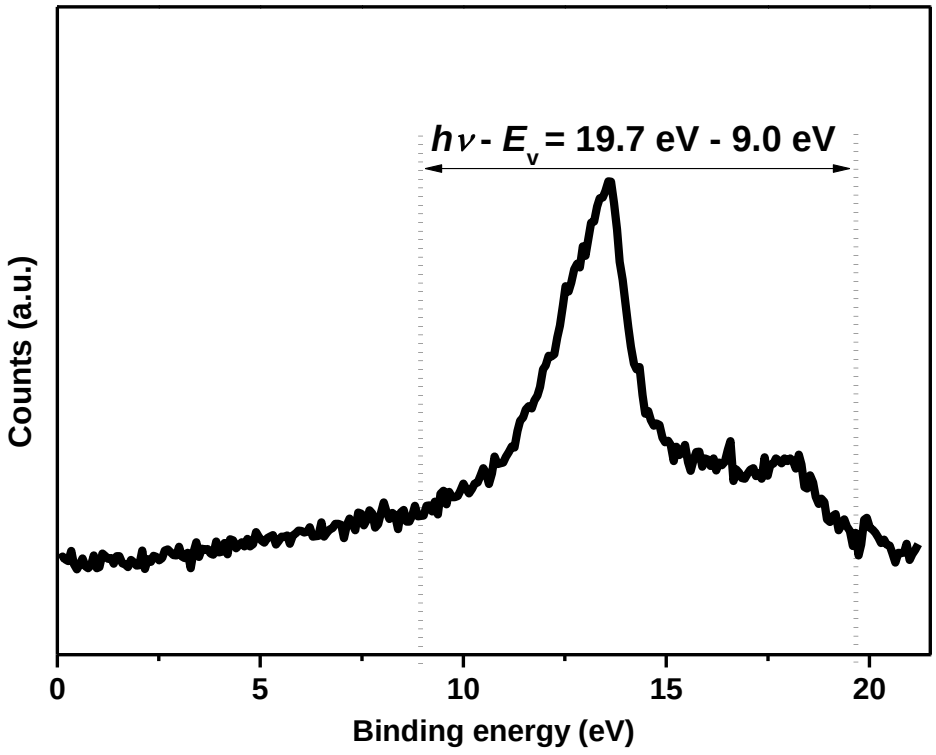

fig. S13. UPS spectrum for ~85-nm sized MgO NPs. UPS spectrum for ~85-nm sized MgO NPs based film (thickness ≈ 0.3 mm) taken with - 8 V bias applied to the sample.